Mol. Cell **44**, 667-678.
14. Yap, K. L., Li, S., Munoz-Cabello, A. M., Raguz, S., Zeng, L., Mujtaba, S., Gil, J., Walsh, M. J. and Zhou, M. M. (2010) Molecular interplay of the noncoding RNA ANRIL and methylated histone H3 lysine 27 by polycomb CBX7 in transcriptional silencing of INK4a. *Mol. Cell* **38**, 662-674.
15. Kotake, Y., Nakagawa, T., Kitagawa, K., Suzuki, S., Liu, N., Kitagawa, M. and Xiong, Y. (2011) Long non-coding RNA ANRIL is required for the PRC2 recruitment to and silencing of p15(INK4B) tumor suppressor gene. *Oncogene* **30**, 1956-1962.
16. Pandey, R. R., Mondal, T., Mohammad, F., Enroth, S., Redrup, L., Komorowski, J., Nagano, T., Mancini-Dinardo, D. and Kanduri, C. (2008) Kcnq1ot1 antisense noncoding RNA mediates lineage-specific transcriptional silencing through chromatin-level regulation. *Mol. Cell* **32**, 232-246.
17. Clemson, C. M., Hutchinson, J. N., Sara, S. A., Ensminger, A. W., Fox, A. H., Chess, A. and Lawrence, J. B. (2009) An architectural role for a nuclear noncoding RNA: NEAT1 RNA is essential for the structure of paraspeckles. *Mol. Cell* **33**, 717-726.
18. Tsai, M. C., Manor, O., Wan, Y., Mosammaparast, N., Wang, J. K., Lan, F., Shi, Y., Segal, E. and Chang, H. Y. (2010) Long noncoding RNA as modular scaffold of histone modification complexes. *Science* **329**, 689-693.
19. Khalil, A. M., Guttman, M., Huarte, M., Garber, M., Raj, A., Rivea Morales, D., Thomas, K., Presser, A., Bernstein, B. E., van Oudenaarden, A., Regev, A., Lander, E. S. and Rinn, J. L. (2009) Many human large intergenic noncoding RNAs associate with chromatin-modifying complexes and affect gene expression. *Proc. Natl. Acad. Sci. U.S.A.* **106**, 11667-11672.
20. Guttman, M., Donaghey, J., Carey, B. W., Garber, M., Grenier, J. K., Munson, G., Young, G., Lucas, A. B., Ach, R., Bruhn, L., Yang, X., Amit, I., Meissner, A., Regev, A., Rinn, J. L., Root, D. E. and Lander, E. S. (2011) lincRNAs act in the circuitry controlling pluripotency and differentiation. *Nature* **477**, 295-300.
21. Kino, T., Hurt, D. E., Ichijo, T., Nader, N. and Chrousos, G. P. (2010) Noncoding RNA gas5 is a growth arrest- and starvation-associated repressor of the glucocorticoid receptor. *Sci. Signal.* **3**, ra8.
22. Redon, S., Reichenbach, P. and Lingner, J. (2010) The non-coding RNA TERRA is a natural ligand and direct inhibitor of human telomerase. *Nucleic Acids Res.* **38**, 5797-5806.
23. Poliseno, L., Salmena, L., Zhang, J., Carver, B., Haveman, W. J. and Pandolfi, P. P. (2010) A coding-independent function of gene and pseudogene mRNAs regulates tumour biology. *Nature* **465**, 1033-1038.
24. Song, M. S., Carracedo, A., Salmena, L., Song, S. J., Egia, A., Malumbres, M. and Pandolfi, P. P. (2011) Nuclear PTEN regulates the APC-CDH1 tumor-suppressive complex in a phosphatase-independent manner. *Cell* **144**, 187-199.
25. Rinn, J. L., Kertesz, M., Wang, J. K., Squazzo, S. L., Xu, X., Brugmann, S. A., Goodnough, L. H., Helms, J. A., Farnham, P. J., Segal, E. and Chang, H. Y. (2007) Functional demarcation of active and silent chromatin domains in human HOX loci by noncoding RNAs. *Cell* **129**, 1311-1323.
26. Yang, Z., Zhou, L., Wu, L. M., Lai, M. C., Xie, H. Y., Zhang, F. and Zheng, S. S. (2011) Overexpression of long non-coding rna hotair predicts tumor recurrence in hepatocellular carcinoma patients following liver transplantation. *Ann. Surg. Oncol.* **18**, 1243-1250.
27. Kogo, R., Shimamura, T., Mimori, K., Kawahara, K., Imoto, S., Sudo, T., Tanaka, F., Shibata, K., Suzuki, A., Komune, S., Miyano, S. and Mori, M. (2011) Long noncoding RNA HOTAIR regulates polycomb-dependent chromatin modification and is associated with poor prognosis in colorectal cancers. *Cancer Res.* **71**, 6320-6326.
28. Kim, K., Jutooru, I., Chadalapaka, G., Johnson, G., Frank, J., Burghardt, R., Kim, S. and Safe, S. (2012) HOTAIR is a negative prognostic factor and exhibits pro-oncogenic activity in pancreatic cancer. *Oncogene* [Epub ahead of print].
29. Niinuma, T., Suzuki, H., Nojima, M., Nosho, K., Yamamoto, H., Takamaru, H., Yamamoto, E., Maruyama, R., Nobuoka, T., Miyazaki, Y., Nishida, T., Bamba, T., Kanda, T., Ajioka, Y., Taguchi, T., Okahara, S., Takahashi, H., Nishida, Y., Hosokawa, M., Hasegawa, T., Tokino, T., Hirata, K., Imai, K., Toyota, M. and Shinomura, Y. (2012) Upregulation of miR-196a and HOTAIR drive malignant character in gastrointestinal stromal tumors. *Cancer Res.* **72**, 1126-1136.
30. Pasmant, E., Laurendeau, I., Heron, D., Vidaud, M., Vidaud, D. and Bieche, I. (2007) Characterization of a germ-line deletion, including the entire INK4/ARF locus, in a melanoma-neural system tumor family: identification of ANRIL, an antisense noncoding RNA whose expression coclusters with ARF. *Cancer Res.* **67**, 3963-3969.
31. Yu, W., Gius, D., Onyango, P., Muldoon-Jacobs, K., Karp, J., Feinberg, A. P. and Cui, H. (2008) Epigenetic silencing of tumour suppressor gene p15 by its antisense RNA. *Nature* **451**, 202-206.
32. Popov, N. and Gil, J. (2010) Epigenetic regulation of the INK4b-ARF-INK4a locus: in sickness and in health. *Epigenetics* **5**, 685-690.
33. Iacobucci, I., Sazzini, M., Garagnani, P., Ferrari, A., Boattini, A., Lonetti, A., Papayannidis, C., Mantovani, V., Marasco, E., Ottaviani, E., Soverini, S., Girelli, D., Luiselli, D., Vignetti, M., Baccarani, M. and Martinelli, G. (2011) A polymorphism in the chromosome 9p21 ANRIL locus is associated to Philadelphia positive acute lymphoblastic leukemia. *Leuk. Res.* **35**, 1052-1059.
34. Pasmant, E., Sabbagh, A., Masliah-Planchon, J., Ortonne, N., Laurendeau, I., Melin, L., Ferkal, S., Hernandez, L., Leroy, K., Valeyrie-Allanore, L., Parfait, B., Vidaud, D., Bieche, I., Lantieri, L., Wolkenstein, P. and Vidaud, M. (2011) Role of noncoding RNA ANRIL in genesis of plexiform neurofibromas in neurofibromatosis type 1. *J. Natl. Cancer Inst.* **103**, 1713-1722.
35. Pasmant, E., Sabbagh, A., Vidaud, M. and Bieche, I. (2011) ANRIL, a long, noncoding RNA, is an unexpected major hotspot in GWAS. *FASEB J.* **25**, 444-448.
36. Ji, P., Diederichs, S., Wang, W., Boing, S., Metzger, R., Schneider, P. M., Tidow, N., Brandt, B., Buerger, H., Bulk, E., Thomas, M., Berdel, W. E., Serve, H. and

Muller-Tidow, C. (2003) MALAT-1, a novel noncoding RNA and thymosin beta4 predict metastasis and survival in early-stage non-small cell lung cancer. *Oncogene* **22**, 8031-8041.
37. Yamada, K., Kano, J., Tsunoda, H., Yoshikawa, H., Okubo, C., Ishiyama, T. and Noguchi, M. (2006) Phenotypic characterization of endometrial stromal sarcoma of the uterus. *Cancer Sci.* **97**, 106-112.
38. Lin, R., Maeda, S., Liu, C., Karin, M. and Edgington, T. S. (2007) A large noncoding RNA is a marker for murine hepatocellular carcinomas and a spectrum of human carcinomas. *Oncogene* **26**, 851-858.
39. Muller-Tidow, C., Diederichs, S., Thomas, M. and Serve, H. (2004) Genome-wide screening for prognosis-predicting genes in early-stage non-small-cell lung cancer. *Lung Cancer* **45(Suppl 2)**, S145-150.
40. Tano, K., Mizuno, R., Okada, T., Rakwal, R., Shibato, J., Masuo, Y., Ijiri, K. and Akimitsu, N. (2010) MALAT-1 enhances cell motility of lung adenocarcinoma cells by influencing the expression of motility-related genes. *FEBS Lett.* **584**, 4575-4580.
41. Tripathi, V., Ellis, J. D., Shen, Z., Song, D. Y., Pan, Q., Watt, A. T., Freier, S. M., Bennett, C. F., Sharma, A., Bubulya, P. A., Blencowe, B. J., Prasanth, S. G. and Prasanth, K. V. (2010) The nuclear-retained noncoding RNA MALAT1 regulates alternative splicing by modulating SR splicing factor phosphorylation. *Mol. Cell* **39**, 925-938.
42. Prensner, J. R., Iyer, M. K., Balbin, O. A., Dhanasekaran, S. M., Cao, Q., Brenner, J. C., Laxman, B., Asangani, I. A., Grasso, C. S., Kominsky, H. D., Cao, X., Jing, X., Wang, X., Siddiqui, J., Wei, J. T., Robinson, D., Iyer, H. K., Palanisamy, N., Maher, C. A. and Chinnaiyan, A. M. (2011) Transcriptome sequencing across a prostate cancer cohort identifies PCAT-1, an unannotated lincRNA implicated in disease progression. *Nat. Biotechnol.* **29**, 742-749.
43. Schneider, C., King, R. M. and Philipson, L. (1988) Genes specifically expressed at growth arrest of mammalian cells. *Cell* **54**, 787-793.
44. Mourtada-Maarabouni, M., Pickard, M. R., Hedge, V. L., Farzaneh, F. and Williams, G. T. (2009) GAS5, a non-protein-coding RNA, controls apoptosis and is downregulated in breast cancer. *Oncogene* **28**, 195-208.
45. Morrison, L. E., Jewell, S. S., Usha, L., Blondin, B. A., Rao, R. D., Tabesh, B., Kemper, M., Batus, M. and Coon, J. S. (2007) Effects of ERBB2 amplicon size and genomic alterations of chromosomes 1, 3 and 10 on patient response to trastuzumab in metastatic breast cancer. *Genes Chromosomes Cancer* **46**, 397-405.
46. Smedley, D., Sidhar, S., Birdsall, S., Bennett, D., Herlyn, M., Cooper, C. and Shipley, J. (2000) Characterization of chromosome 1 abnormalities in malignant melanomas. *Genes Chromosomes Cancer* **28**, 121-125.
47. Luo, J. H., Ren, B., Keryanov, S., Tseng, G. C., Rao, U. N., Monga, S. P., Strom, S., Demetris, A. J., Nalesnik, M., Yu, Y. P., Ranganathan, S. and Michalopoulos, G. K. (2006) Transcriptomic and genomic analysis of human hepatocellular carcinomas and hepatoblastomas. *Hepatology* **44**, 1012-1024.
48. Petrovics, G., Zhang, W., Makarem, M., Street, J. P., Connelly, R., Sun, L., Sesterhenn, I. A., Srikantan, V., Moul, J. W. and Srivastava, S. (2004) Elevated expression of PCGEM1, a prostate-specific gene with cell growth-promoting function, is associated with high-risk prostate cancer patients. *Oncogene* **23**, 605-611.
49. Srikantan, V., Zou, Z., Petrovics, G., Xu, L., Augustus, M., Davis, L., Livezey, J. R., Connell, T., Sesterhenn, I. A., Yoshino, K., Buzard, G. S., Mostofi, F. K., McLeod, D. G., Moul, J. W. and Srivastava, S. (2000) PCGEM1, a prostate-specific gene, is overexpressed in prostate cancer. *Proc. Natl. Acad. Sci. U.S.A.* **97**, 12216-12221.
50. Braconi, C., Valeri, N., Kogure, T., Gasparini, P., Huang, N., Nuovo, G. J., Terracciano, L., Croce, C. M. and Patel, T. (2011) Expression and functional role of a transcribed noncoding RNA with an ultraconserved element in hepatocellular carcinoma. *Proc. Natl. Acad. Sci. U.S.A.* **108**, 786-791.
51. Calin, G. A., Liu, C. G., Ferracin, M., Hyslop, T., Spizzo, R., Sevignani, C., Fabbri, M., Cimmino, A., Lee, E. J., Wojcik, S. E., Shimizu, M., Tili, E., Rossi, S., Taccioli, C., Pichiorri, F., Liu, X., Zupo, S., Herlea, V., Gramantieri, L., Lanza, G., Alder, H., Rassenti, L., Volinia, S., Schmittgen, T. D., Kipps, T. J., Negrini, M. and Croce, C. M. (2007) Ultraconserved regions encoding ncRNAs are altered in human leukemias and carcinomas. *Cancer Cell* **12**, 215-229.
52. Khaitan, D., Dinger, M. E., Mazar, J., Crawford, J., Smith, M. A., Mattick, J. S. and Perera, R. J. (2011) The melanoma-upregulated long noncoding RNA SPRY4-IT1 modulates apoptosis and invasion. *Cancer Res.* **71**, 3852-3862.
53. Yu, M., Ohira, M., Li, Y., Niizuma, H., Oo, M. L., Zhu, Y., Ozaki, T., Isogai, E., Nakamura, Y., Koda, T., Oba, S., Yu, B. and Nakagawara, A. (2009) High expression of ncRAN, a novel non-coding RNA mapped to chromosome 17q25.1, is associated with poor prognosis in neuroblastoma. *Int. J. Oncol.* **34**, 931-938.
54. Zhu, Y., Yu, M., Li, Z., Kong, C., Bi, J., Li, J. and Gao, Z. (2011) ncRAN, a newly identified long noncoding RNA, enhances human bladder tumor growth, invasion and survival. *Urology* **77**, 510.e1-5.
55. Chung, S., Nakagawa, H., Uemura, M., Piao, L., Ashikawa, K., Hosono, N., Takata, R., Akamatsu, S., Kawaguchi, T., Morizono, T., Tsunoda, T., Daigo, Y., Matsuda, K., Kamatani, N., Nakamura, Y. and Kubo, M. (2011) Association of a novel long non-coding RNA in 8q24 with prostate cancer susceptibility. *Cancer Sci.* **102**, 245-252.
56. Matouk, I. J., DeGroot, N., Mezan, S., Ayesh, S., Abu-lail, R., Hochberg, A. and Galun, E. (2007) The H19 non-coding RNA is essential for human tumor growth. *PLoS One* **2**, e845.
57. Gabory, A., Ripoche, M. A., Yoshimizu, T. and Dandolo, L. (2006) The H19 gene: regulation and function of a non-coding RNA. *Cytogenet. Genome Res.* **113**, 188-193.
58. Zhou, Y., Zhong, Y., Wang, Y., Zhang, X., Batista, D. L., Gejman, R., Ansell, P. J., Zhao, J., Weng, C. and Klibanski, A. (2007) Activation of p53 by MEG3 non-coding RNA. *J. Biol. Chem.* **282**, 24731-24742.
59. Zhang, X., Gejman, R., Mahta, A., Zhong, Y., Rice, K. A., Zhou, Y., Cheunsuchon, P., Louis, D. N. and Klibanski, A.

(2010) Maternally expressed gene 3, an imprinted noncoding RNA gene, is associated with meningioma pathogenesis and progression. *Cancer Res.* **70**, 2350-2358.
60. Wang, J., Liu, X., Wu, H., Ni, P., Gu, Z., Qiao, Y., Chen, N., Sun, F. and Fan, Q. (2010) CREB up-regulates long non-coding RNA, HULC expression through interaction with microRNA-372 in liver cancer. *Nucleic Acids Res.* **38**, 5366-5383.
61. Panzitt, K., Tschernatsch, M. M., Guelly, C., Moustafa, T., Stradner, M., Strohmaier, H. M., Buck, C. R., Denk, H., Schroeder, R., Trauner, M. and Zatloukal, K. (2007) Characterization of HULC, a novel gene with striking up-regulation in hepatocellular carcinoma, as noncoding RNA. *Castroenterology* **132**, 330-342.
62. Tomlins, S. A., Aubin, S. M., Siddiqui, J., Lonigro, R. J., Sefton-Miller, L., Miick, S., Williamsen, S., Hodge, P., Meinke, J., Blase, A., Penabella, Y., Day, J. R., Varambally, R., Han, B., Wood, D., Wang, L., Sanda, M. G., Rubin, M. A., Rhodes, D. R., Hollenbeck, B., Sakamoto, K., Silberstein, J. L., Fradet, Y., Amberson, J. B., Meyers, S., Palanisamy, N., Rittenhouse, H., Wei, J. T., Groskopf, J. and Chinnaiyan, A. M. (2011) Urine TMPRSS2:ERG fusion transcript stratifies prostate cancer risk in men with elevated serum PSA. *Sci. Transl. Med.* **3**, 94ra72.

see related editorial on page 470

A Novel Pit Pattern Identifies the Precursor of Colorectal Cancer Derived From Sessile Serrated Adenoma

Tomoaki Kimura, MD[1,7], Eiichiro Yamamoto, MD, PhD[2,3,7], Hiro-o Yamano, MD[1], Hiromu Suzuki, MD, PhD[2,3], Seiko Kamimae, MD[2], Masanori Nojima, MD, PhD, MPH[4], Takeshi Sawada, MD, PhD[2], Masami Ashida, MS[2], Kenjiro Yoshikawa, MD[1], Ryo Takagi, MD, PhD[1], Ryusuke Kato, MD[1], Taku Harada, MD[1], Ryo Suzuki, MD[1,3], Reo Maruyama, MD, PhD[2,3], Masahiro Kai, PhD[2], Kohzoh Imai, MD, PhD[5], Yasuhisa Shinomura, MD, PhD[3], Tamotsu Sugai, MD, PhD[6] and Minoru Toyota, MD, PhD[2]

OBJECTIVES: **Sessile serrated adenomas (SSAs) are known to be precursors of sporadic colorectal cancers (CRCs) with microsatellite instability (MSI), and to be tightly associated with *BRAF* mutation and the CpG island methylator phenotype (CIMP). Consequently, colonoscopic identification of SSAs has important implications for preventing CRCs, but accurate endoscopic diagnosis is often difficult. Our aim was to clarify which endoscopic findings are specific to SSAs.**

METHODS: **The morphological, histological and molecular features of 261 specimens from 226 colorectal tumors were analyzed. Surface microstructures were analyzed using magnifying endoscopy. Mutation in *BRAF* and *KRAS* was examined by pyrosequencing. Methylation of *p16*, *IGFBP7*, *MLH1* and *MINT1*, *-2*, *-12* and *-31* was analyzed using bisulfite pyrosequencing.**

RESULTS: **Through retrospective analysis of a training set ($n=145$), we identified a novel surface microstructure, the Type II open-shape pit pattern (Type II-O), which was specific to SSAs with *BRAF* mutation and CIMP. Subsequent prospective analysis of an independent validation set ($n=116$) confirmed that the Type II-O pattern is highly predictive of SSAs (sensitivity, 65.5%; specificity, 97.3%). *BRAF* mutation and CIMP occurred with significant frequency in Type II-O-positive serrated lesions. Progression of SSAs to more advanced lesions was associated with further accumulation of aberrant DNA methylation and additional morphological changes, including the Type III, IV and V pit patterns.**

CONCLUSIONS: **Our results suggest the Type II-O pit pattern is a useful hallmark of the premalignant stage of CRCs with MSI and CIMP, which could serve to improve the efficacy of colonoscopic surveillance.**

SUPPLEMENTARY MATERIAL is linked to the online version of the paper at http://www.nature.com/ajg

Am J Gastroenterol 2012; 107:460–469; doi:10.1038/ajg.2011.457; published online 10 January 2012

INTRODUCTION

Colorectal cancers (CRCs) arise through the accumulation of multiple genetic changes to oncogenes and tumor suppressor genes, a process often referred to as the adenoma–carcinoma sequence (1). In addition to genetic changes, epigenetic alterations such as DNA methylation also have important roles in silencing cancer-related genes, and a subset of CRCs show hypermethylation of the promoter CpG islands of multiple genes (2,3). This has been termed the CpG island methylator phenotype (CIMP) (3). CRCs with CIMP have several characteristic features, including frequent *BRAF* mutation, *MLH1* methylation, microsatellite instability (MSI) and infrequent *p53* mutation (4–6).

Serrated lesions were initially described by Longacre and Fenoglio-Preiser (7) and include hyperplastic polyps (HPs), sessile serrated adenomas (SSAs) and traditional serrated adenomas (TSAs). The criteria used to categorize serrated lesions as HPs, TSAs or SSAs were defined by Torlakovic *et al.* (8) and Snover *et al.* (9), but distinction between SSAs and HPs is often difficult because of their morphological similarity (10–12). In the past, SSAs were classified as HPs, which were considered to have no malignant potential. However, recent studies have shown that SSAs are mainly observed in the proximal colon and are associated with frequent *BRAF* mutation and CIMP, which suggests SSAs are precursors of CRCs with MSI. By contrast, TSAs are

[1]Department of Gastroenterology, Akita Red Cross Hospital, Akita, Japan; [2]Department of Molecular Biology, Sapporo Medical University, Sapporo, Japan; [3]First Department of Internal Medicine, Sapporo Medical University, Sapporo, Japan; [4]Department of Public Health, Sapporo Medical University, Sapporo, Japan; [5]Division of Novel Therapy for Cancer, The Advanced Clinical Research Center, The Institute of Medical Science, The University of Tokyo, Tokyo, Japan; [6]Department of Pathology, Iwate Medical University, Morioka, Japan; [7]These authors contributed equally to this work. **Correspondence:** Hiromu Suzuki, MD, PhD, Department of Molecular Biology, Sapporo Medical University, S1, W17, Chuo-ku, Sapporo 060-8556, Japan. E-mail: hsuzuki@sapmed.ac.jp
Received 21 June 2011; accepted 15 September 2011

often found in the distal colon and show frequent *KRAS* mutation (13–16).

Colonoscopic identification of serrated lesions and conventional adenomas has important implications for preventing CRCs. However, accurate diagnosis of serrated lesions is often difficult, and it is particularly difficult to distinguish SSAs from HPs solely through colonoscopic observation (12,17). In that regard, high-resolution magnifying colonoscopy is now recognized to be a powerful diagnostic tool for predicting the malignancy of conventional adenomas, the efficacy of which has been confirmed in a number of independent studies (18–21). According to Kudo's classification (18,20), the pit patterns of non-neoplastic lesions are classified as Type I (normal colon) or II (HP), whereas the pit patterns of neoplastic lesions are classified as Types III, IV and V. Because Type II pits are indicative of non-neoplastic HP lesions and are also observed in serrated lesions, SSAs and TSAs were considered to be benign when the pit pattern classification was established (17,22,23). But given the aforementioned evidence that SSAs may be precursors of CRCs with MSI, it would seem necessary to refine the criteria for the Type II pit pattern, based on its histological and molecular characteristics.

In the present study, we hypothesized that SSAs exhibit morphological features that are distinct from the features of non-neoplastic lesions or conventional adenomas. To test that idea, we carried out an integrative analysis of the morphological, histological and molecular features of serrated lesions with the ultimate aim of establishing more accurate diagnostic criteria.

METHODS

Patients and tissue specimens

All specimens of colorectal serrated lesions were collected from Japanese patients who underwent endoscopic mucosal resection of a colorectal tumor at Akita Red Cross Hospital. The training set included 145 specimens from 122 serrated lesions or conventional adenomas collected between January 2009 and December 2009. An independent validation set included 116 specimens from 104 serrated lesions or conventional adenomas, which were prospectively collected between January 2010 and December 2010. Informed consent was obtained from all patients before collection of the specimens. Approval of this study was obtained from the Institutional Review Board of Akita Red Cross Hospital and Sapporo Medical University. Genomic DNA was extracted from biopsy specimens using the standard phenol-chloroform procedure.

Endoscopic analysis

High-resolution magnifying endoscopes (CF260AZI; Olympus, Tokyo, Japan) were used for all colonoscopic analyses. Participating in this study were 10 endoscopists, all of whom were trained as gastroenterologists for at least 3 years. Among them, moreover, four had experience with more than 1,000 cases before this study. All serrated lesions detected by colonoscopy were observed at high magnification, using indigo carmine dye. Surface microstructures were classified according to the Kudo's pit pattern classification system (18,20). Biopsy specimens were obtained from all of the lesions for genomic DNA extraction, after which the lesions were treated by endoscopic mucosal resection or endoscopic submucosal dissection. In principle, one biopsy specimen was obtained from each lesion. If more than two pit patterns were observed in a single lesion, a biopsy specimen was obtained from each pit pattern portion.

Histological analysis

Histological findings for all specimens were evaluated by a gastrointestinal pathologist (TS) who was blinded to the clinical and molecular information. Conventional adenoma was diagnosed using the standard criteria. Conventional adenoma with serration (Ad+se) was included with the serrated lesions (15). Serrated lesions (HPs, SSAs and TSAs) were classified on the basis of the criteria previously described by Torlakovic *et al.* (8). In this study, serrated lesions that did not satisfy the criteria for SSA or TSA were defined as intermediate (IM) and classified in the same category as HP (HP/IM). Mixed serrated lesions composed of HP/IM, SSA, TSA, adenomatous change (Ad-C) or high-grade dysplasia (HGD) were evaluated on the basis of each component and described as HP/IM + Ad-C, SSA + Ad-C or SSA + HGD.

DNA methylation analysis

CpG island methylation was analyzed as described previously (24). Briefly, genomic DNA (1 μg) was modified with sodium bisulfite using an EpiTect Bisulfite Kit (QIAGEN, Hilden, Germany). Pyrosequencing was carried out using a PSQ96 system with a PyroGold reagent Kit (QIAGEN), and the results were analyzed using Q-CpG software (QIAGEN). A cutoff value of 15% was used to define genes as methylation-positive. Tumors were defined as CIMP-positive when methylation was detected in three or more loci of the five markers (*MINT1*, *MINT2*, *MINT12*, *MINT31* and *p16*). Sequence information for primers and probes are summarized in **Supplementary Table 1**.

Mutation analysis

Mutation of codon 600 of *BRAF* and codons 12 and 13 of *KRAS* was examined by pyrosequencing using *BRAF* and *KRAS* pyro kits (QIAGEN) according to the manufacturer's instructions.

Analysis of MSI

MSI was assessed as described previously (25). The primers proposed by the National Cancer Institute Workshop on Microsatellite Instability (BAT25, BAT26, D5S346, D2S123, D17S250) were used (26). MSI was defined by the presence of abnormally sized bands in the tumor sample, as compared with a sample of the corresponding normal DNA. A tumor sample was defined as MSI-positive when two or more markers showed instability.

Statistical analysis

To compare differences in continuous variables between groups, a *t*-test or ANOVA with *post-hoc* Tukey test was performed. Fisher's exact test or χ^2-test was used for analysis of categorical data. Odds ratios were calculated using logistic regression models. Values of $P < 0.05$ (two-sided) were considered significant. Receiver operating characteristic curves for diagnosis of colorectal

tumors with *BRAF* mutations and CIMP were constructed, based on the probability in each leaf of the decision tree. All statistical analyses were carried out using SPSS statistics 18 (IBM Corporation, Somers, NY).

RESULTS

Type II open-pit pattern is a specific feature of SSAs

To achieve a more accurate colonoscopic diagnosis of SSAs, we first examined the pit patterns in a series of histologically defined serrated lesions ($n=69$) and conventional adenomatous lesions ($n=76$) as a training set (**Supplementary Figure 1**). Through this retrospective study, we identified an interesting pit pattern that was specific to SSAs (**Figure 1**). We termed this pattern Type II-open (Type II-O), because it was similar to the conventional Type II pattern, but the pits were wider and more rounded in shape, reflecting dilatation of the crypts. The shapes of the Type II-O pits also differed from those of Type I pits, in that they were larger in size with serrations surrounding the pit. Lesions with Type II-O pits often showed conventional Type II pits in the surrounding fields.

We categorized the lesions into two groups, depending upon the presence of Type II-O pits, and then examined the relationship between the Type II-O pit pattern and several molecular alterations (**Table 1**). Importantly, none of the conventional adenomas exhibited the Type II-O pit pattern, and among the serrated lesions, the Type II-O pit pattern was specific to SSAs. A majority of Type II-O pit-positive lesions exhibited *BRAF* mutations, whereas *KRAS* mutations were more prevalent among Type II-O-negative lesions (**Table 1**). Because *BRAF* mutation is strongly associated with CIMP in CRCs, we determined the CIMP status of the lesions by assessing the methylation of five CIMP markers (*MINT1*, *-2*, *-12*, *-31* and *p16*). As expected, a majority of the lesions with Type II-O pits was CIMP-positive, and showed elevated levels of *p16* methylation (**Table 1**, **Figure 2**). Type II-O-positive lesions also showed elevated methylation of *IGFBP7*, another CIMP-associated gene (**Figure 2**) (27).

To confirm our findings, we carried out a prospective study using an independent validation set, which included serrated lesions ($n=55$) and conventional adenomas ($n=61$; **Supplementary Figure 1**). With this validation set, we initially made a colonoscopic diagnosis of each lesion, and then examined its histological and molecular features. Again, we observed that Type II-O pits were specific to SSAs with *BRAF* mutations and CIMP (**Table 1**). As shown in **Figure 2**, lesions with Type II-O pits exhibited elevated levels of *p16* and *IGFBP7* methylation. These results strongly suggest that morphological observations made using magnifying colonoscopy can effectively identify one of the earliest steps in the CIMP and MSI pathway.

Clinicopathological features of Type II-O-positive lesions

The clinicopathological characteristics of the patients are summarized in **Table 2**. There were no statistically significant differences

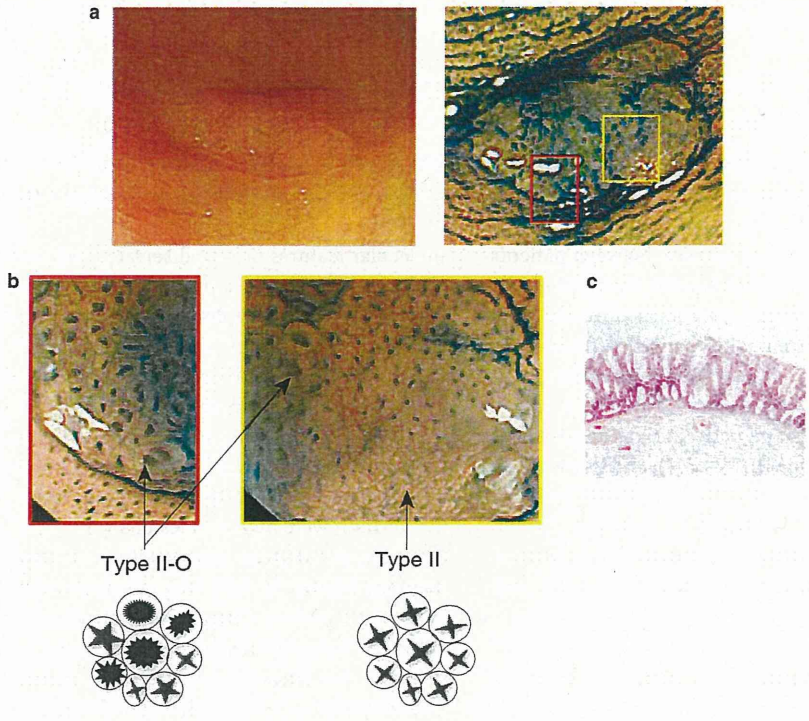

Figure 1. Identification of the Type II open-shape (Type II-O) pit pattern in sessile serrated adenomas (SSAs). (**a**) Colonoscopic view of a representative SSA with (right) and without indigo carmine dye (left). (**b**) Magnified views of the SSA areas indicated by the red and yellow boxes in panel **a**. Left panel: the majority of the pits are Type II-O. Right panel: the upper region is covered by Type II-O pits, whereas the lower region is covered by conventional Type II pits. Schematic diagrams of Type II and Type II-O pits are shown below. (**c**) Histological appearance of the SSA with Type II-O pits.

Table 1. Association of the Type II-O pattern with histological and molecular features

	SSA		*KRAS*		*BRAF*		CIMP	
	Yes	No	Mut	WT	Mut	WT	Positive	Negative
(a) Training Set								
Serrated lesions								
Type II-O								
Positive	15	0	1	14	14	1	11	4
Negative	0	31	9	22	9	22	3	28
Conventional adenoma								
Type II-O								
Positive	0	0	0	0	0	0	0	0
Negative	0	76	25	51	1	75	2	74
Sensitivity	1.000		0.029		0.583		0.688	
Specificity	1.000		0.839		0.99		0.962	
(b) Validation Set								
Serrated lesions								
Type II-O								
Positive	19	2	1	20	18	3	15	6
Negative	10	12	4	18	10	12	5	17
Conventional adenoma								
Type II-O								
Positive	0	0	0	0	0	0	0	0
Negative	0	61	16	45	1	60	1	60
Sensitivity	0.655		0.001		0.621		0.714	
Specificity	0.973		0.759		0.960		0.928	
OR (95% CI)	69.4 (14–343.5)		0.2 (0.0–1.2)		39.3 (9.9–155.7)		32.1 (9.1–113.1)	

CI, confidence interval; CIMP, CpG island methylator phenotype; Mut, mutant; OR, odds ratio; SSA, sessile serrated adenoma; Type II-O, Type II open-shape; WT, wild type.

with respect to age, lesion morphology and size between patients with Type II-O pit-positive and -negative lesions. In addition, the majority of lesions with Type II-O pits were located on the right side of the colon, which is consistent with the well-defined characteristics of CIMP-positive CRCs. Histologically, a large majority of Type II-O pit-positive lesions were diagnosed as SSA. A subset of lesions exhibited more advanced pit patterns in addition to the Type II-O pits (Type II-O plus Type III, IV or V), and those specimens showed mixtures of SSA and Ad-C, TSA or HGD (**Table 2**). By contrast, a majority of the conventional Type II lesions showed HP/IM histology, and a subset of Type II lesions that contained additional Type IV patterns showed a mixture of HP/IM and Ad-C or TSA (**Table 2**).

Molecular signatures define the progression of Type II-O-positive serrated lesions

Our observations summarized above suggest that serrated lesions with Type II-O pits differ from those with conventional Type II pits, and that they represent a premalignant stage of CIMP-positive CRCs. To confirm this hypothesis, we next examined in detail the molecular features of mixed serrated lesions in which Type II or II-O pits were present along with more advanced pits (Type III, IV or V; **Figure 3a-d**, **Supplementary Figure 2**). In lesions with Type II-O plus Type IV or V pits, both the Type II-O subcomponents and the Type IV or V subcomponents exhibited similar molecular features (e.g., *BRAF* mutation and CIMP), though they differed histologically (i.e., SSAs in the Type II-O components vs. TSAs, Ad-Cs or HGDs in the Type IV or V components; **Figure 3e**, **Supplementary Table 2**). In addition, levels of *p16* and *MLH1* methylation were higher in lesions with Type II-O pits plus more advanced pits than in lesions with only Type II-O pits (**Supplementary Figure 3**). MSI was observed only in portions with a Type V pit pattern (**Supplementary Figure 2**, **Supplementary Table 2**). These molecular signatures strongly suggest that Type IV and V subcomponents develop from coexisting SSAs.

In contrast to lesions with Type II-O pits, those without Type II-O pits showed much lower frequencies of *BRAF* mutation and CIMP, but higher frequencies of *KRAS* mutations (**Figure 3e**, **Supplementary Table 2**). And although Type II-O pit-negative lesions with advanced pit patterns (e.g., Type II plus Type IV lesions) did

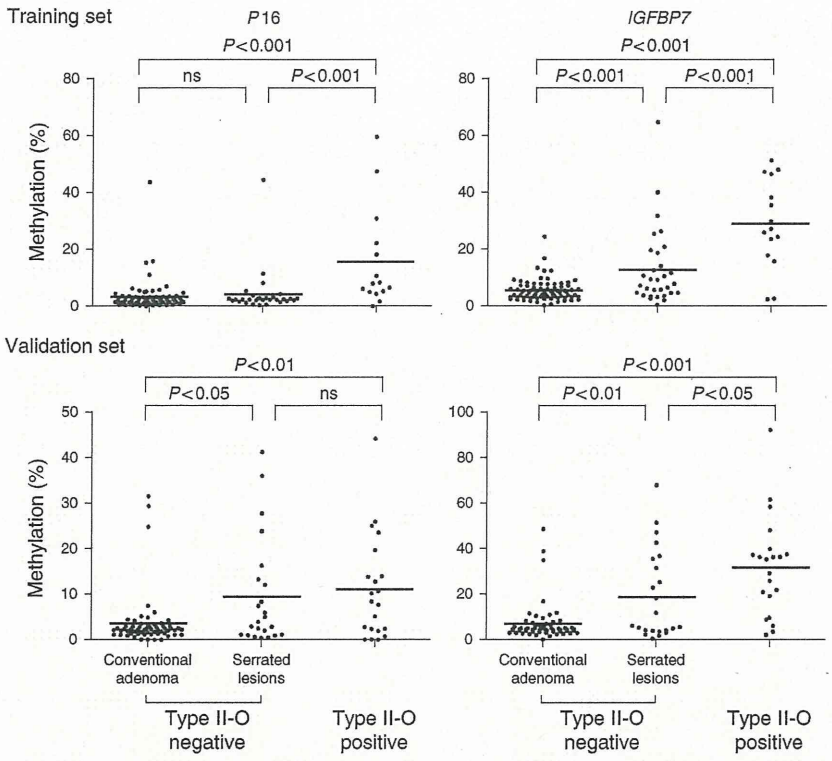

Figure 2. Increased CpG island methylation in Type II open-shape (Type II-O) pit-positive lesions. All of the Type II-O pit-positive specimens are serrated lesions. Type II-O pit-negative specimens contain serrated lesions and conventional adenomas. Methylation levels of *p16* and *IGFBP7* were obtained by bisulfite pyrosequencing. Each point represents an individual specimen; the horizontal bars represent the respective means.

show somewhat higher frequencies of *BRAF* mutation and CIMP, they never showed MSI (**Figure 3e**, **Supplementary Table 2**). Thus, Type II-O pit-positive and -negative serrated lesions appear to develop through distinct tumorigenic pathways.

To develop an efficient diagnostic method for detecting precursors of *BRAF* mutant and CIMP-positive CRCs, we next constructed a diagnostic tree to classify serrated lesions on the basis of their pit patterns (**Figure 4a**). We first excluded lesions containing only advanced pits (Type III or more) because they are unlikely to be SSAs. We next divided the lesions according to whether they were Type II-O pit-positive or -negative as the second node of the diagnostic tree. Finally, we subdivided the lesions into four groups according to the coexisting advanced pits (**Figure 4a; Supplementary Table 3**). As shown in **Figure 4a**, group 1 (Type II-O plus Type III, IV or V) exhibited significant specificity for *BRAF* mutation and CIMP-positive lesions. To evaluate the performance of the diagnostic tree in defining *BRAF*-mutant plus CIMP-positive lesions, a receiver operating characteristic curve was constructed by plotting the sensitivity over one specificity at three cut-offs for each group (group 1 vs. groups 2–4; groups 1–2 vs. groups 3–4; groups 1–3 vs. group 4). Areas under the curves in both the training set and the validation set were very high (for training set, 0.987; for validation set, 0.846).

We summarize our findings in **Figure 5**. We found that the Type II-O pit pattern is a clinically useful hallmark of SSAs. Moreover, during the progression of carcinogenesis, SSAs undergo additional molecular and histological changes, and our results demonstrate that colonoscopic observations can be used to predict these changes.

DISCUSSION

SSAs were previously reported to be precursors of CRCs with MSI (13,14). Although identification of SSAs in screening colonoscopies has important implications for the prevention and early detection of CRCs, the colonoscopic findings for SSAs have been less than definitive. Criteria for colonoscopic diagnosis of colorectal lesions were established on the basis of histological findings; however, there is no clear histological definition to distinguish SSAs from HPs, and the rate of concordance among gastrointestinal pathologists for diagnosis of SSA is low (10). Detection of SSAs also reportedly differs among endoscopists, and classification of HP and SSA differs among pathologists (12).

In the present study, we performed an integrated analysis of the genetic, epigenetic and clinical features of serrated lesions in an effort to establish more definitive criteria for the colonoscopic diagnosis of SSA. We identified an SSA-specific pit pattern Type II-O and prospectively validated its clinical utility for detecting SSA. Molecular dissection of mixed serrated lesions suggested that subcomponents with advanced pit patterns were derived from coexisting Type II-O pit-positive SSAs, and additional molecular

Table 2. Clinicopathological features of the patients

	Training Set			Validation Set		
	Type II-O			Type II-O		
	Positive	Negative	*P*-value	Positive	Negative	*P*-value
Age (mean±s.d.)	71.4±7.84	68.7±10.09	NS	65.48±8.77	64.05±10.72	NS
Sex						
F (%)	9 (60)	29 (27.1)	0.013	10 (47.62)	34 (40.96)	NS
M (%)	6 (40)	78 (72.9)		11 (52.38)	49 (59.04)	
Location						
Right (%)	14 (93.33)	43 (40.19)	<0.001	18 (85.71)	44 (53.01)	0.002
Left (%)	1 (6.67)	28 (26.17)		3 (14.46)	27 (32.53)	
Rectum (%)	0 (0)	36 (33.64)		0 (0)	12 (14.46)	
Morphology						
Flat (%)	7 (46.67)	49 (45.79)	NS	15 (71.43)	43 (51.81)	NS
Flat+protruded (%)	6 (40)	13 (12.15)		2 (9.52)	4 (5.82)	
Protruded (%)	2 (13.33)	45 (42.06)		4 (19.05)	36 (43.37)	
Size (mm, mean±s.d.)	11.00±4.02	10.45±8.56	NS	11.71±6.02	13.83±10.73	NS
Pit pattern						
Type II (%)		19 (19.92)			16 (19.28)	
Type II+Type IV (%)		13 (12.26)			6 (7.23)	
Type IV (%)		53 (50)			34 (40.96)	
Type III (%)		21 (19.81)			26 (31.33)	
Type III+Type IV (%)		0 (0)			1 (1.2)	
Type II-O (%)	6 (40.00)			16 (76.2)		
Type II-O+Type III (%)	0 (0)			2 (9.52)		
Type II-O+Type IV (%)	7 (46.67)			2 (9.52)		
Type II-O+Type V (%)	2 (13.33)			1 (4.76)		
Histology						
HP/IM (%)	0 (0)	14 (13.08)	<0.001	1(4.76)	4 (4.82)	<0.001
HP/IM+Ad-C (%)	0 (0)	0 (0)		0 (0)	2 (2.40)	
HP/IM+TSA (%)	0 (0)	9 (8.41)		1(4.76)	2 (2.41)	
TSA (%)	0 (0)	6 (5.61)		0 (0)	2 (2.41)	
Ad+se (%)	0 (0)	2 (1.87)		0 (0)	2 (2.41)	
Ad (%)	0 (0)	76 (71.03)		0 (0)	61 (73.49)	
SSA (%)	8 (53.33)	0 (0)		17 (80.95)	8 (9.64)	
SSA+Ad-C (%)	4 (26.67)	0 (0)		1 (4.76)	2 (2.41)	
SSA+HGD (%)	2 (13.33)	0 (0)		1 (4.76)	0 (0)	
SSA+TSA (%)	1 (6.67)	0 (0)		0 (0)	0 (0)	

Ad, conventional adenoma; Ad-C, adenomatous change; Ad+se, conventional adenoma with serration; HGD, high grade dysplasia; HP/IM, hyperplastic polyp/intermediate; NS, not significant; SSA, sessile serrated adenoma; TSA, traditional serrated adenoma; Type II-O, Type II open-shape.

alterations (e.g., *p16* and *MLH1* methylation) were acquired during tumorigenesis. The inactivation of cell cycle regulatory genes, including *p16* and *p53*, has an important role in CRC development by enabling tumor cells to escape oncogene-induced cellular senescence (28,29). *IGFBP7* has been shown to have a central role in oncogenic *BRAF*-induced senescence, and it is also a direct

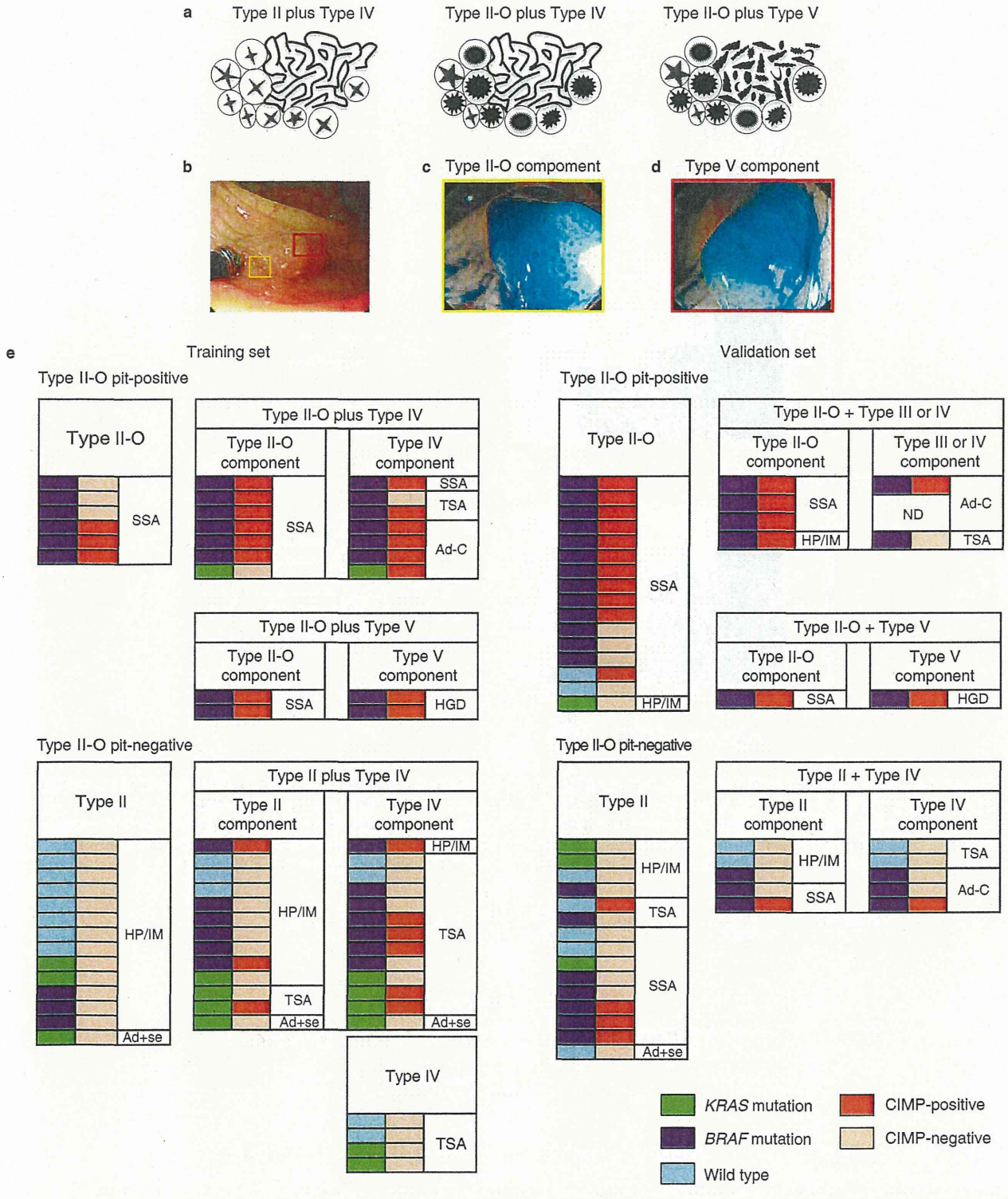

Figure 3. *Morphological and molecular signatures reveal progression of sessile serrated adenomas* (SSAs) *with Type II open-shape* (*Type II-O pits*). (**a**) Schematic diagram of serrated lesions with mixed pit patterns. (**b**) Colonoscopic view of a representative serrated lesion with Type II-O and Type V pits. (**c**, **d**) Magnified views of the Type II-O subcomponent (**c**) indicated by the yellow box (**b**) and the Type V subcomponent (**d**) indicated by the red box (**b**). (**e**) Summary of the molecular, colonoscopic and histological features of serrated lesions with or without Type II-O pits. Each row indicates one lesion. Results of the training set are on the left, and those of the validation set are on the right. ND, not determined.